Talanta 131 (2015) 541–547

Contents lists available at ScienceDirect

Talanta

journal homepage: www.elsevier.com/locate/talanta

Influence of Pluronic F127 on the distribution and functionality of inkjet-printed biomolecules in porous nitrocellulose substrates

Liyakat Hamid Mujawar [a,b,*], Aart van Amerongen [a,**], Willem Norde [b,c]

[a] Food and Biobased Research, Biomolecular Sensing and Diagnostics, Wageningen University and Research Centre, Bornse Weilanden 9, 6708 AA Wageningen, The Netherlands
[b] Laboratory of Physical Chemistry and Colloid Science, Wageningen University, Dreijenplein 6, 6703 HB Wageningen, The Netherlands
[c] University Medical Center Groningen, University of Groningen, A. Deusinglaan 1, 9713 AV Groningen, The Netherlands

ARTICLE INFO

Article history:
Received 29 April 2014
Received in revised form
30 July 2014
Accepted 2 August 2014
Available online 12 August 2014

Keywords:
Inkjet printing
Pluronic
Spot morphology
Nitrocellulose
Orientation

ABSTRACT

The distribution of inkjet-printed biomolecules in porous nitrocellulose substrates often results in a non-homogeneous spot morphology commonly referred to as 'doughnut-shaped' spots. We have studied the influence of Pluronic F127 (an amphiphilic surfactant) on the functionality of inkjet-printed primary antibody molecules and on the final assay result by performing a one-step antibody binding assay in the nitrocellulose substrate. The primary antibody was printed with and without Pluronic, followed by the addition of double-labelled amplicons as antigen molecules and a fluorophore-labelled streptavidin as detection conjugate. The distribution of the fluorescence intensity down into the nitrocellulose substrate was investigated by confocal laser scanning microscopy in 'Z' stacking mode. Each horizontal slice was further analysed by applying a concentric ring format and the fluorescence intensity in each slice was represented in a colour-coded way. The mean and total fluorescence intensity of the antibody binding assay (fluorescent streptavidin) showed a peak at 0.2% (w/v) Pluronic F127. In addition, an improved spot morphology was observed also peaking at the same Pluronic concentration. Subsequently, we investigated the direct influence of Pluronic F127 on the location of the primary antibody molecules by labelling these molecules with the fluorophore Alexa-488. Our results show that upon increasing the concentration of Pluronic F127 in the printing buffer, the spot diameter increased and the number of primary antibody molecules bound in the spot area gradually decreased. This was confirmed by analysing the distribution of fluorescently labelled primary antibody molecules down into the membrane layers.

We conclude that a particular ratio between primary antibody and Pluronic F127 molecules in combination with available substrate binding capacity results in an optimal orientation, that is F*ab*-UP, of the primary antibody molecules. Consequently, an increased number of antigen molecules (in our case the labelled amplicons) and of the fluorescent detection conjugate (streptavidin) will give an optimal signal. Moreover, distribution of the primary antibody molecules was more homogeneous at the optimal Pluronic F127 concentration, contributing to the better spot morphology observed.

1. Introduction

Non-contact arraying is a modern tool for printing biomolecules [1] on a range of porous and non-porous substrates. Researchers have shown that high-quality microarrays are produced on porous substrates like nitrocellulose [2,3], porous silicon [4], alumina [5–7] and hydrogels [8] as compared the non-porous substrates like glass [9] and polystyrene [10]. On porous substrates, a lower limit of detection can be obtained as compared to non-porous substrates[11]. The 3-D matrix of the porous substrates [12] enables more molecules to bind as projected per unit surface area and this results in a better signal-to-noise (S/N) ratio [13]. Of all the available porous substrates, the nitrocellulose membrane has been used extensively in diagnostic applications [2,14–16] and for producing biochips[3,17].

It has been commonly observed that, upon printing, biomolecules often distribute non-homogeneously which results in 'doughnut-shaped' spots, also referred to as the 'coffee-stain' effect[18–20]. Researchers have successfully demonstrated that

* Corresponding author. Present address: Center of Excellence in Environmental Studies, King Abdulaziz, University, P.O. Box 80216, Jeddah 21589, Saudi Arabia.
** Corresponding author. Tel.: +31 317 480 164; fax: +31 317 483 011.
E-mail addresses: Liyakat.mujawar@gmail.com (L. Hamid Mujawar), Aart.vanamerongen@wur.nl (A. van Amerongen), Willem.Norde@wur.nl (W. Norde).

http://dx.doi.org/10.1016/j.talanta.2014.08.001
0039-9140/

for DNA microarrays, incorporation of various additives like DMSO [21], polyvinyl alcohol[22], betaine[23] and Triton-X 100[24] can result in a more homogeneous spot morphology. However, the chemical aspects of DNA microarrays cannot be easily translated to the production of protein microarrays due to the fundamental biophysical and biochemical differences between these two classes of biological substances.

Recently, Norde and Lyklema have shown that Pluronic molecules enhance the functionality of deposited antibodies by forcing them to adsorb at the substrate surface with their antigen binding sites oriented towards the solution[25]. They have also reported that in the presence of Pluronic (P75), the adsorbed IgG molecules showed both improved stability and biological activity. Pluronics are tri-block copolymers with repeating polyoxyethylene-polyoxypropylene-polyoxyethylene (PEO-PPO-PEO) units where the central part (PPO) is hydrophobic and the ends (PEO) are hydrophilic in nature. For our study, we have used Pluronic F-127 which belongs to a class of polymers called as poloxamers [26].

However, Pluronic P75 is very different from Pluronic F127 used by us. Earlier studies performed by Alexandridis *et al.* [27] have shown significant difference in the properties of the two classes of tri-block polymers. More specifically, the molar mass of F127 is 12600 Da whereas that of P75 is 4150 Da and the percentage of PEO in F127 is 70% whereas in P75 it is only 50%. This corresponds to $(PEO)_{100}$-$(PPO)_{65}$-$(PEO)_{100}$ for F127 and $(PEO)_{24}$-$(PPO)_{36}$-$(PEO)_{24}$ for P75, the subscripts indicating the average number of monomers in the polymer blocks. Thus the two Pluronics differ strongly in length of the respective PPO and PEO blocks. The larger PPO block in F127 allows this Pluronic to attach more strongly to the substratum surface and, more importantly, the longer PEO moieties in F127 allows for a much stronger influence on the orientation of IgG molecules on the substratum surface (see Sections 3.1 and 3.3). On the other hand, Pluronic F127 has been used for inkjet printing applications [28,29] of protein microarrays. Wolter *et al.* have successfully demonstrated that the application of Pluronic F127 improves the signal as well as the limit of detection on a 2-D substrate surface [30]. Therefore, we have selected Pluronic F127 for studying its influence on the functionality of inkjet-printed primary antibody molecules, the final assay result, spot morphology as well as the distribution of biomolecules in nitrocellulose membrane pads.

We have assessed the influence of various concentrations of Pluronic F127 (0 to 1% (w/v)) on the spot morphology and functionality of the primary antibody (anti-FITC). Using a non-contact inkjet printer, primary anti-FITC antibodies were printed on nitrocellulose membrane slides, and the functionality of the primary antibodies was investigated by performing a one-step diagnostic antibody assay based on the binding of a double-labelled amplicon (FITC- and biotin-labelled), as was reported for the nucleic acid microarray immunoassay (NAMIA) [2,9,10]. The distribution as well as the functionality of the primary antibody was judged from the distribution of the fluorescence signal of the final assay (i.e. fluorescent streptavidin). Using confocal laser scanning microscopy, the NAMIA spots were sliced horizontally ('Z' stack method) and the signal distribution profile in each slice was calculated using a concentric ring format. The results are presented in a colour-coded format. Additionally, we also investigated the direct influence of the amphiphilic surfactant (Pluronic F127) on the distribution of the primary antibody molecules that had been labelled with Alexa-488.

2. Material and methods

2.1. Reagents

Pluronic F127 was purchased from Sigma Aldrich (St. Louis, MO, USA), and a 1% (w/v) stock solution was prepared in 150 mM phosphate buffered saline (PBS, pH 7.4). Running buffer (100 mM borate buffer containing 1% BSA and 0.05% Tween-20) was used as a diluent for the conjugates/labels and also during the intermediate washing steps.

2.2. Biomolecules

Anti-fluoroisothiocynate (FITC) was purchased from Bioconnect (Huissen, The Netherlands). The DNA templates for *Corynebacterium bovis* were provided bythe Animal Health Service, Deventer, The Netherlands. Streptavidin-Alexa-633 for labelling biotinylated amplicons was from Invitrogen (Bleiswijk, The Netherlands).

2.3. Substrates for printing biomolecules

Nexterion nitrocellulose membrane coated slides in 16-pad format were purchased from Schott AG (Mainz, Germany). The dimension of each pad was 6×6 mm, whereas the thickness was ~ 11 μm.

2.4. Labelling of the primary anti-FITC antibody

The primary anti-FITC antibody molecules were labelled with Alexa-488 fluorophore using an Alexa-Fluor 488 antibody labelling kit (Invitrogen, Oregon, USA). The labelling procedure was carried out as described by Invitrogen, and the concentration of the fluorophore-conjugated antibody (anti-FITC-Alexa-488) was measured using a Nanodrop-1000-v3.6 spectrophotometer (Wilmington, DE, USA).

2.5. Printing of antibodies on NC membrane slides

Anti-FITC and Alexa-488 conjugated anti-FITC antibodies were diluted (200 $\mu g mL^{-1}$) in various Pluronic F127 concentrations (0%, 0.01%, 0.05%, 0.1%, 0.2%, 0.4, 0.8% 1.0%w/v) and loaded into the wells of a Genetix microplate (384 wells). The diluted antibodies were printed on the nitrocellulose membrane pads using a non-contact inkjet printer, sciFLEXARRAYER S3 (Scienion AG, Berlin, Germany). The printer was placed in a hood to maintain constant temperature and humidity. Spotting of the biomolecules was performed at room temperature and $70 \pm 1\%$ humidity. The voltage and pulse of the piezo-dispensing capillary (PDC) were optimized to print a droplet of ~ 250 pL throughout the experiment. The slides were stored overnight in a sealed Al pouch.

2.6. PCR reaction

DNA template from *Corynebacterium bovis* was amplified using primers Cb-F2 and Cb-R3 according to a published protocol[10]. The PCR protocol was optimized to 30 minutes using Phire Hot Start polymerase (Finnzymes) and the Piko thermal cycler (Finnzymes). The forward primer was labelled with a FAM tag and the reverse primer with biotin. The amplification resulted in a double stranded amplicon with at each end a tag, FAM or biotin. Gel electrophoresis confirmed that the amplicon obtained after PCR had the correct band length[31].

2.7. Nucleic acid microarray immunoassay (NAMIA)

To investigate the influence of Pluronic F127 in the printing buffer of the primary anti-FITC antibody a one-step diagnostic assay was performed on the NC membrane slides based on the principle of the Nucleic Acid Microarray Immuno Assay, NAMIA [2,9,10]. Anti-FITC antibodies (specific for the FAM tag) were diluted in various concentrations of Pluronic F127 and printed onto the NC membrane slides. Prior to performing NAMIA, the NC

membrane pads were incubated with running buffer (1 h) as a blocking step. The test was performed as a short incubation (60 min) of the PCR amplicon containing the FAM and the biotin labels and streptavidin-Alexa-633 (see Fig. 1). The final washing was performed with running buffer (two times) followed by rinsing with MQ water. The fluorescence intensity of the signal was related to the functionality of the primary anti-FITC antibody molecules with respect to the Pluronic F127 concentration in the printing buffer.

2.8. Confocal laser scanning microscopy (CLSM)

The spot morphology and the distribution of the biomolecules in the porous NC membranes were analysed by confocal laser scanning microscopy (CLSM; Carl Zeiss Axiovert 200 microscope, Zeiss, Jena, Germany), equipped with a LSM 5 Exciter. The fluorophore-labelled spots were first scanned at a 10x magnification (overall surface fluorescence), where the configuration of the objective was LD Plan-Neofluar 10x/0.30 Korr M27. For Alexa-633 conjugated NAMIA spots, the He-Ne laser set at 633 nm was used, whereas for the Alexa-488 conjugated anti-FITC antibodies, an Ar laser set at 488 nm was used. The size of the pinhole was 182 μm and the transmission was 11%. The dimension of the scanner was X: 1270 μm and Y: 1270 μm. The detector gain values for Alexa-633 and Alexa-488 were 850 and 700, respectively. The gain values were chosen such that no background was obtained for the scanned spot. Using LSM software, the mean intensity, that is the mean intensity per pixel, was calculated per spot. The average of the mean intensities of four NAMIA spots was determined, and data plots were represented along with the standard deviation. For other purposes, the total fluorescence intensity (product of mean intensity and spot pixel area) was used.

The distribution of the fluorescence intensity down into the NC membrane was studied by 'Z' stacking using an oil-immersion lens (100x magnification). The transmission of He-Ne laser (633 nm) was 24%. The configuration of the objective was LD Plan-Neofluar 100x/0.6 Korr Ph2 M27 and the dimensions of the scanner were X: 127.0 μm, Y: 127.0 μm, Z: 11.03 μm respectively. The pinhole diameter was adjusted to 1.02 μm such that each spot of biomolecule on NC membranes was sliced horizontally into 12 slices with a thickness of 1 μm per slice (Fig. 2-A). Such slicing technique has been already used in the past to investigate the penetration of colloidal ink in paper substrates[32] and to study the distribution of antibodies in NC membrane slides[33,34]. Furthermore, each slice was divided in five concentric-rings (the thickness of each ring was constant and was equal to the radius of the inner ring). The mean intensity of each ring was determined to assess the (in)-homogeneity of the spots (Fig. 2-B). Earlier, Mujawar *et al.* have demonstrated that the interpretation of 'Z' stack data in a colour-coded format gave a clear overview of the distribution of the biomolecules in 3-D substrates [34].

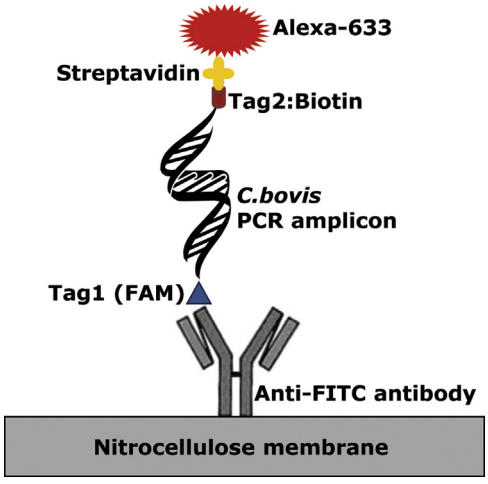

Fig. 1. Schematic representation for detection principle of NAMIA.

3. Results and discussion

3.1. Influence of Pluronic F127in the printing buffer of the primary anti-FITC antibody molecules on the final diagnostic assay signal

In order to investigate the influence of Pluronic F127 on the functionality of the primary anti-FITC antibody, a diagnostic antibody assay was performed based on the principle of NAMIA (see Fig. 1) [9,10]. The final assay signal was scored on the basis of the fluorescence of the bound secondary conjugate, streptavidin. With increasing concentration of Pluronic in the printing buffer, the spot radii of the NAMIA spots also increased from 58 to 83 μm (see Fig. 3, panel I-A). The property of a surfactant to enhance the spreading and uniform distribution of a droplet on a substrate surface has also been reported by Dugas *et al.* [35]. They showed that during evaporation of a droplet in the presence of surfactant, the hydrodynamic flow causes the accumulation of the surface-active agents at the periphery of the droplet. This increased concentration lowers the evaporation on the edge of the droplet, thus assisting in an uniform spot deposition throughout the droplet area.

The fluorescence intensity of the assay spots was influenced by the concentration of Pluronic. In the absence of Pluronic (i.e. only PBS in the printing buffer of the primary antibody), the fluorescence signal intensity was low and the spot morphology was doughnut-like (see Fig. 3, panel I-B,C). However, in the presence of Pluronic in the printing buffer, the mean and total fluorescence intensity increased and the doughnut spot morphology was substantially suppressed when the Pluronic concentration was increased to 0.2%. A further increase in the concentration of Pluronic up to 0.4% resulted in a similar spot morphology, but the mean and total fluorescence intensity of the spot was less than that observed for the 0.2% spot. At 1% Pluronic, the fluorescence intensity of the spot was almost vanished (see Fig. 3, panel I-B,C). Wolter *et al.* [30] also observed a similar enhancement in the signal due to incorporation of Pluronic

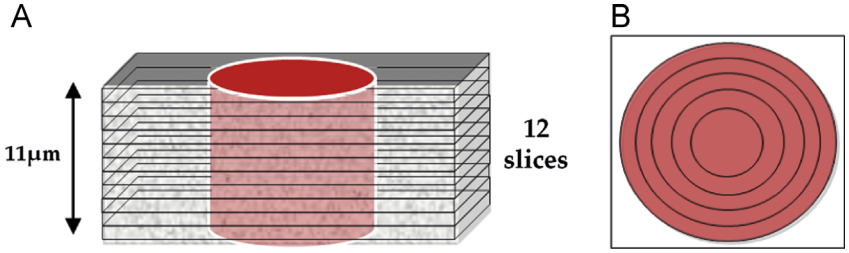

Fig. 2. (A) Schematic representation of the 'Z' stacking method. (B) Schematic view of the five concentric ring model to calculate the distribution of the mean intensity of the concentric rings in each slice of the spot.

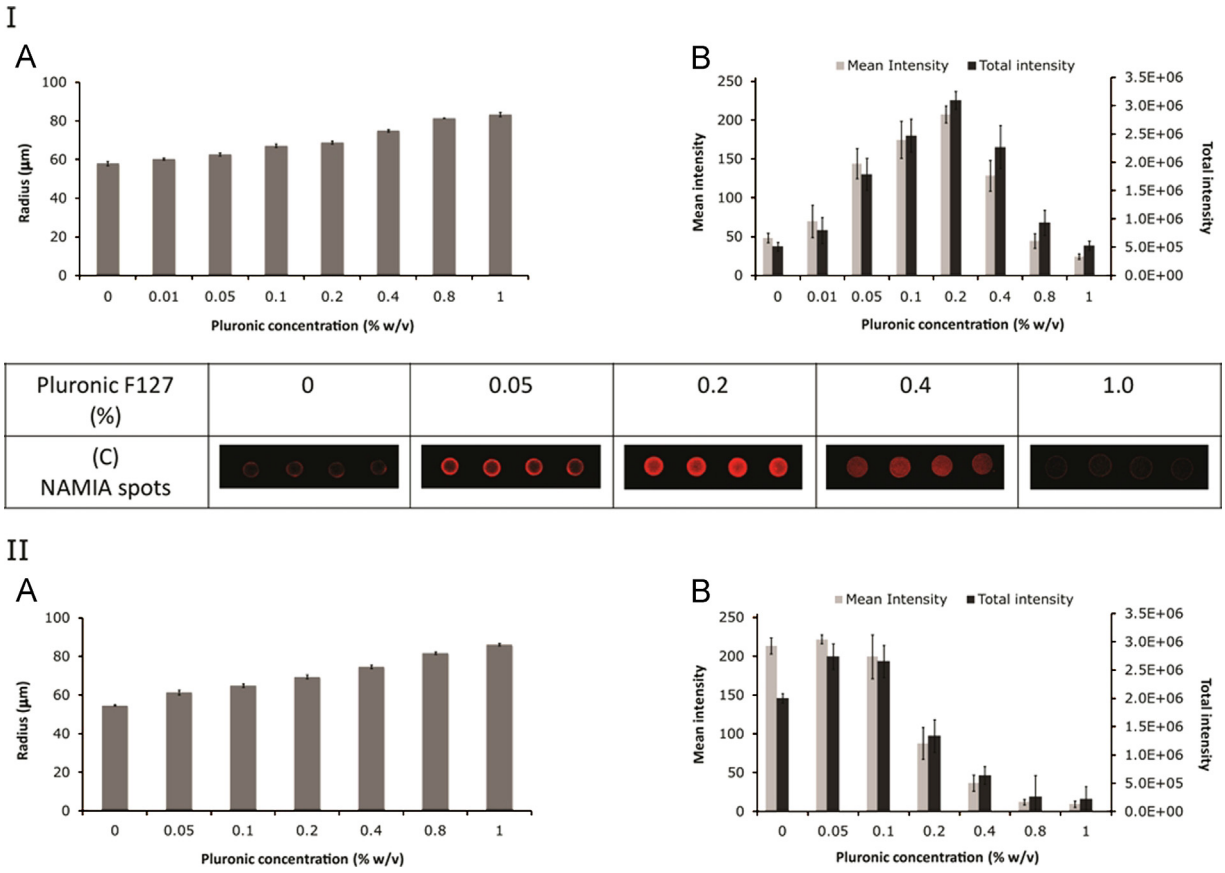

Fig. 3. Panel I shows the influence of Pluronic F127 on the final spot radius upon printing the primary anti-FITC antibody with Pluronic F127 (A) and on the mean and total fluorescence signal intensity, Strep-Alexa-633 (B) of the diagnostic assay. In C, CLSM (10x) images of the assay spots are shown. Panel II shows the spot radius (A) and the mean and total fluorescence (B) of the fluorescently-labelled primary antibody molecules (Alexa-488).

F127. The signal enhancement on a non-porous substrate was mainly due to improved stabilization of protein molecules in the presence of Pluronic F127. However, they noticed excessive spreading of the spots on non-porous substrates, which was further improved by addition of trehalose. We have used a similar approach for improvement of the signal on porous substrate but in addition to this we also studied the distribution of the diagnostic assay signal into the three dimensional matrix of the nitrocellulose substrate and the possible mechanism for signal improvement.

3.2. Influence of Pluronic F127 on the fluorescence signal distribution in a porous substrate and the final signal of the antibody assay ('Z' stack analysis)

Based on the fluorescent dye attached, we also demonstrated the distribution of the primary anti-FITC antibody molecules down into the NC membrane using a 'Z' stacking mode (slicing of the spots) of the CLSM (100x magnification). This kind of slicing technique to study the distribution of the inkjet-printed antibodies down into the NC substrate has been used in the past by Lieshout *et al.* and Mujawar *et al.* [33,34]. In addition, we applied a concentric ring model to measure the fluorescence in rings across the spot in order to assess its morphology, as demonstrated by Mujawar *et al.* [34].

In the absence of Pluronic F127, the distribution of the fluorescence intensity (i.e. assay signal) of the spot in the subsequent slices was non-homogeneous, thus resembling a doughnut-shape distribution, that is higher intensity at the edges than in the centre. As indirectly judged from the final spot fluorescence, it was also observed that in the absence of the amphiphilic surfactant, the biomolecule penetrates only up to 6 μm deep in the NC membrane (see Fig. 4, panel I). This shows that upon inkjet printing, most of the NC volume beneath the spot was still unoccupied by any biomolecule. Similar observations were reported by Mujawar *et al.* who showed that the substrate properties of NC membrane slides (hydrophobicity/hydrophilicity, wettability) play an important role in the distribution and penetration depth of antibody molecules and also influence the functionality of these inkjet-printed biomolecules [34]. The low fluorescence signals in the absence of Pluronic in the slices just below the surface could be well explained by unfavourable orientations of the antibody molecules that restrict the accessibility of the antigen-binding sites by the antigen [36].

Incorporation of Pluronic (0.01%) in the printing buffer resulted in an increase of the fluorescence intensity of the final assay spot in each slice, along with deeper penetration of the antibody molecules into the membrane. With a further increase in the Pluronic concentration (0.05% and 0.1%), the fluorescence intensity in the horizontal slices not only increased, but was also found to be more homogeneously distributed. The best homogeneously distributed fluorescence intensity distribution was observed throughout all the slices of the assay spots when the anti-FITC antibody was printed with 0.2% Pluronic. Based on the NAMIA spot images and 'Z' stack data, it can be concluded that the distribution of biomolecules in the spots was less homogeneous in the absence of Pluronic F127 as compared to the spots of primary antibodies printed with 0.2% Pluronic (see Fig. 3, panel I-C and Fig. 4, panel I).

A further increase in the Pluronic concentration resulted in spots with a diameter larger than the dimensions of the CLSM scanner, frustrating 'Z' stacking analysis at 100x magnification for

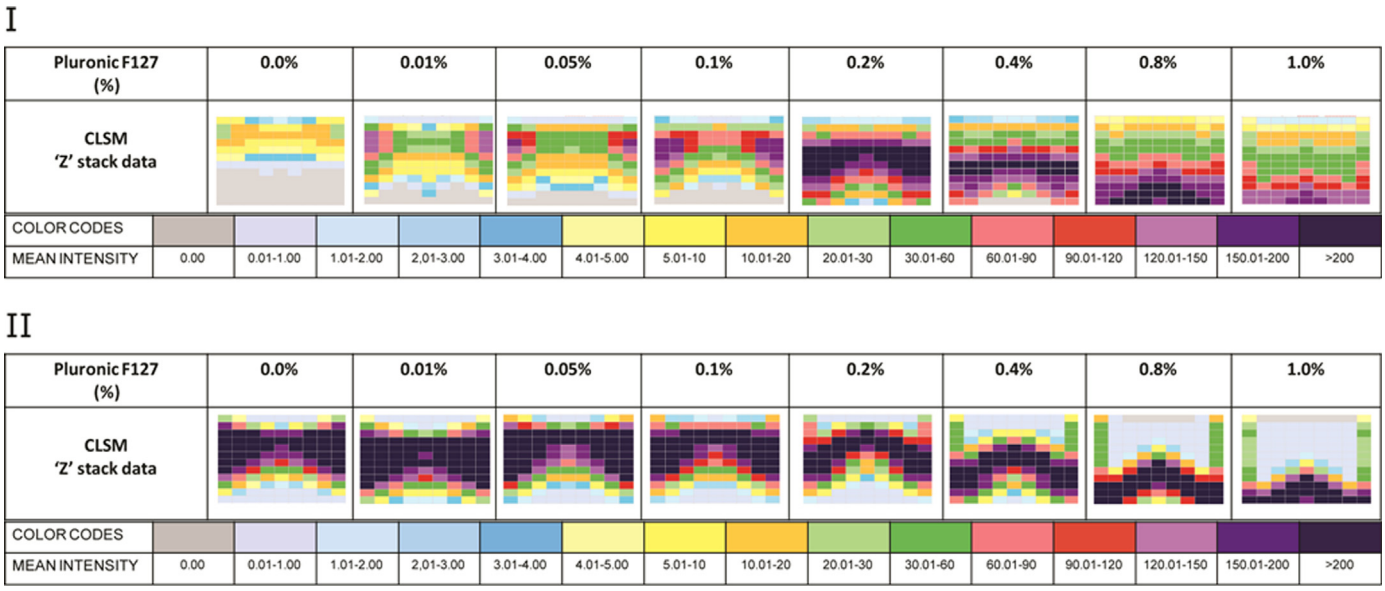

Fig. 4. Influence of Pluronic F127 on the distribution and functionality of primary antibody molecules. Panel I shows the CLSM (100x) 'Z' stack data in colour-coded format of the distribution of the fluorescent signal (Strep-Alexa-633) of the diagnostic assay in 1 μm layers. Panel II shows the CLSM (100x) 'Z' stack data of the distribution of the fluorescently-labelled primary antibody molecules (Alexa-488).

the spots printed with higher Pluronic concentration (i.e. above 0.2%). Even then, we have provided the 'Z' stacks data for the spots printed with 0.4%, 0.8% and 1.0% Pluronic, but limited to the same dimensions as those used for the spots printed with 0.2% Pluronic and lower. As the concentration increases, the biomolecules present in the liquid droplet not only spread horizontally (X-Y) on the NC substrate (see Fig. 3, panel I-A), but also penetrates deeper in the vertical (Z) direction (Fig. 4, panel I). The spreading of liquid droplets in a porous substrate is three-dimensional as compared to a non-porous substrate, onto which it is only two-dimensional. In the presence of surfactant the biomolecules in the liquid droplet spread more homogeneously on non-porous substrates, which is a well-studied phenomenon [35,37].

We also observed that in the absence of Pluronic (i.e. 0% (w/v)) the printed biomolecules were confined to the upper layers of the membrane, indicating a very rapid binding of antibody molecules to the upper nitrocellulose fibres. However, on these porous NC substrates and with increasing Pluronic concentration, the biomolecules penetrated deeper into the NC matrix, that is into layers beneath and outside the visible spot area. The 'Z' stack colour-coded data shows that at higher Pluronic concentration ($>$ 0.2%) less fluorescence (i.e. the fluorescence in the 1 μm NC slices) was observed, whereas the higher fluorescent signals showed up in deeper layers of the membrane. Since the thickness of the NC membrane is only 11 μm and at higher concentrations of the tri-block copolymer molecules binding to the nitrocellulose fibres, the primary antibody molecules most probably were forced to deeper layers of the membrane and to regions outside the spot area as analysed by the Z-stack method. Since the fluorescence signal at deeper layers of the membrane will be weaker as recorded from above the membrane (10x magnification), the final assay signal will be lower at higher Pluronic F127 concentrations, which is indeed the case as shown in Fig. 3, panel I-B and in line with the distribution of the fluorescent signal in the membrane layers as shown in Fig. 4, panel I.

3.3. *Influence of Pluronic F127 on the distribution and functionality of the primary antibody molecules*

In order to investigate whether the explanation of a lower final fluorescent assay signal upon Pluronic F127 concentrations above 0.2%, the effect of Pluronic 127 on the binding of the primary antibody molecules was determined. We printed Alexa-488 conjugated primary anti-FITC antibody molecules in various Pluronic concentrations. The NC membrane pads were rinsed twice with running buffer and finally with MQ water. After air drying, the spots of IgG-Alexa-488 on NC pads were scanned (10x) to analyse the total spot fluorescence at various Pluronic concentrations. With increasing concentration of Pluronic, the spot radii of the Alexa-488 conjugated primary anti-FITC antibody molecules also increased (see Fig. 3, panel II-A) as was observed for the final assay spots (compare with Fig. 3, panel I-A). However, the fluorescence intensity of the Alexa-488 conjugated primary antibody molecules was highest in the absence of Pluronic and continued to decrease with increasing Pluronic concentration; an inverse relationship was observed between Pluronic concentration and the mean fluorescence intensity (see Fig. 3, panel II-B). However, the total fluorescence intensity slightly increased when the Pluronic concentration was raised from 0% to 0.05%, but beyond 0.05% the trend for the total fluorescence intensity was similar to that observed for the mean intensity. When the concentration of Pluronic was 0% and 0.05%, the mean intensity was highest whereas for higher Pluronic concentration (up to 1%), the fluorescence intensity was very low. The decrease in the mean and total intensity with increasing Pluronic concentration (Fig. 3, panel II-B), strongly implies that Pluronic F127 molecules itself do not increase (or enhance) the fluorescence intensity of a fluorophore. Pluronics are known to form layers at solid-liquid interfaces where the PPO part have strong affinity to the surface [38]. A recent study by Mohanty *et al.* showed that Pluronic F127 does not result in fluorescence quenching [39]. Increasing the Pluronic concentration up to 20% did not quench the fluorescence signal of the fluorophore (8-anilino-1-naphthalene-sulfonic acid (ANS)). Moreover, the application of the amphiphilic surfactant in pharmacokinetic studies showed a higher fluorescence by the increased uptake of drug molecules upon increasing the concentration of Pluronic molecules [40,41]. From these studies, it can be concluded that the results we observed were not due to the influence of Pluronic F127 molecules on fluorescent signals.

To further investigate the influence of Pluronic molecules, we decided to determine the distribution of the primary Alexa-488 labelled antibodies using the 'Z' stacking mode (slicing of the spots) of the CLSM (100x magnification). In Fig. 4, panel II, it can be

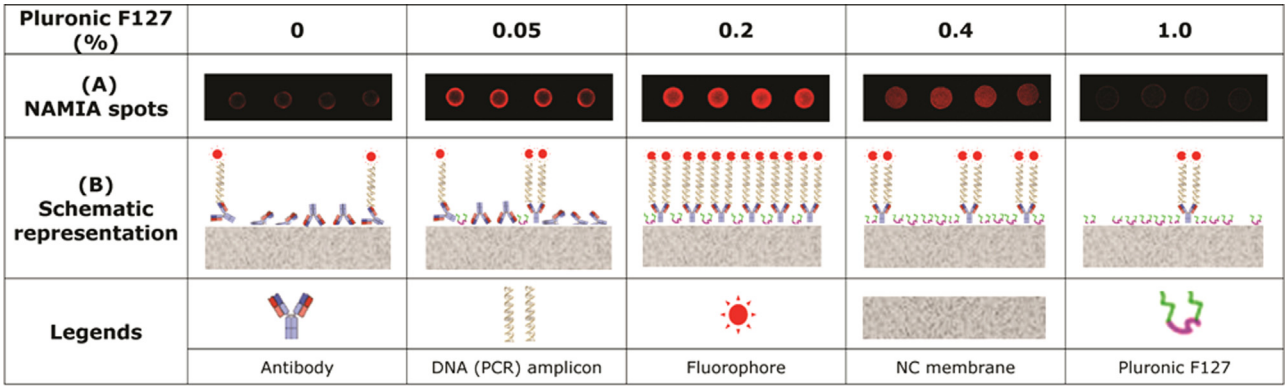

Fig. 5. A schematic illustration to explain the optimal diagnostic assay performance at 0.2% Pluronic F127.

seen that the fluorescence distribution is quite similar for the primary antibodies printed with 0 up to 0.1% Pluronic F127. However, at 0.2% the distribution started to differ, especially at the edges of the spots where the higher fluorescent signals was observed in lower layers. A further increase in the Pluronic concentration shifted the higher fluorescent signals even deeper down in the membranes. This observation coincides with the gradual decrease of the total fluorescence as resulting from printed fluorescently-labelled primary antibody molecules (see Fig. 3, panel II-B.

Comparison of data in Fig. 3, panel I-B and II-B and Fig. 4, panel I and II shows that at 0.2% the printed primary antibody molecules are less in number in the spot area (as judged from the total spot fluorescence) but are obviously highly functional. From our results, we have to conclude that the presence of Pluronic in the printing buffer has an effect on the functionality of the primary antibody molecules. Apparently, a particular ratio between primary antibody and Pluronic F127 molecules in combination with available substrate binding capacity in the spot area triggers an optimal orientation of the primary antibody molecules. Consequently, an increased number of antigen molecules (in our case the labelled amplicons) and, hence, of the fluorescent detection conjugate (streptavidin-Alexa-633) will bind, resulting in the highest total signal. Moreover, the distribution of the primary antibody molecules was more homogeneous at the optimal Pluronic F127 concentration, contributing to the better spot morphology observed.

In any immunoassay, the correct orientation of the antibody molecule is crucial as it plays a role in defining the final assay signal. The primary antibodies upon printing on NC membranes may adopt 'Side-ON', 'Flat-ON', 'F*ab*-UP' and 'F*ab*-DOWN' orientations [25,42]. When the antibody molecule deposits in a Side-ON or Flat-ON orientation and, even more so, in a *Fab*-DOWN orientation, fewer F*ab* binding sites are available for binding antigen molecules. However, in the F*ab*-UP orientation maximum accessibility of the antigen binding sites is ensured [36]. Thus, in the absence of Pluronic, the printed anti-FITC antibody molecules may orient themselves more or less randomly at the NC surface, that is in any of the before mentioned orientations. In the presence of Pluronic, this polymer competes with the antibody molecules for binding to the substrate surface. Consequently, the density of the antibody molecules at and under the spot is lowered, which would result in a reduced fluorescence intensity of the anti-FITC assay. However, because the Pluronic molecules tend to bind to the surface through their central apolar PPO part, leaving their two terminal polar PEO parts dangling in the solution, antibody molecules most likely dock in the interstitial spaces between the adsorbed Pluronic molecules. At a particular Pluronic concentration, these interstitial spaces are confined such that they prohibit Side-ON, Flat-ON and F*ab*-DOWN orientations of the antibodies, but allow accommodation of the less bulky part of the antibody molecule, its Fc part, resulting in a F*ab*-UP orientation [25]. Docking of the Fc part of the IgG molecule into the PEO layer will more easily occur when the thickness of the brush (~5.5 nm for Pluronic F127) [43] does not exceed the length of Fc part (7.7 nm) [44]. Thus, the adsorbed Pluronic molecules may act as a sieve to force the antibody molecules to adsorb via their Fc part and with their binding sites away from the surface, leaving the F*ab* binding sites available for binding the antigen molecules. The interaction of the protein molecules with the PEO brushes has been discussed in detail by Norde *et al.* [25,45]. This sieving effect and, hence, the fluorescence intensity of the assay is enhanced with increasing coverage of the NC surface by Pluronic up to a certain degree (i.e. 0.2%) beyond which the Pluronic molecules are too densely packed to allow for sufficient antibody molecules to be incorporated (i.e. 0.4% and higher). As a result, a lower fluorescence intensity of the assay spots was observed when the Pluronic concentration was 0.4% and higher.

The proposed role of Pluronic in assisting IgG molecules has been schematically illustrated in Fig. 5, which most probably explains the differences observed in the fluorescence signals between spots of which the primary anti-FITC antibody was printed with different concentrations of Pluronic F127.

4. Conclusions

Incorporation of the amphiphilic surfactant, Pluronic F127, at a particular concentration in the printing buffer improves the functionality and also the distribution of primary antibodies in porous NC substrates. CLSM data (10x) confirmed that in the presence of Pluronic F127, a more homogeneous morphology was obtained and that the biomolecules distributed more uniformly down into the NC membrane (confirmed by 'Z' stack analysis). A diagnostic assay on top of these primary antibodies with antigen and fluorophore-labelled streptavidin showed that the mean fluorescence intensity was best at a concentration of 0.2% Pluronic F127 in the printing buffer. It is concluded that at this optimal concentration, Pluronic F127 molecules induced the preferred orientation of the primary antibody molecules, that is F*ab*-UP, resulting in an improved final assay signal.

Acknowledgements

This research is supported by the Dutch Technology Foundation STW, Applied-Science Division of NWO (Dutch Organisation for Scientific Research) and the Technology Program of the Ministry of Economic Affairs of The Netherlands

References

[1] J.B. Delehanty, F.S. Ligler, Anal. Chem. 74 (2002) 5681–5687.
[2] P.S. Noguera, G.A. Posthuma-Trumpie, M. van Tuil, F.J. van der Wal, A.d. Boer, A. P.H.A. Moers, A. van Amerongen, Anal. Chem 83 (2011) 8531–8536.
[3] L.H. Mujawar, A. Moers, W. Norde, A. Van Amerongen, Anal. Bioanal. Chem 405 (2013) 7469–7476.
[4] A. Ressine, G.r. Marko-Varga, T. Laurell, M.R. El-Gewely, Porous silicon protein microarray technology and ultra-/superhydrophobic states for improved bioanalytical readout, in: Biotechnology Annual Review, Elsevier (2007) 149–200.
[5] S.Y. Kim, J. Yu, S.J. Son, J. Min, Ultramicroscopy 110 (2010) 659–665.
[6] Y. Wu, P. de Kievit, L. Vahlkamp, D. Pijnenburg, M. Smit, M. Dankers, D. Melchers, M. Stax, P.J. Boender, C. Ingham, N. Bastiaensen, R. de Wijn, D. van Alewijk, H. van Damme, A.K. Raap, A.B. Chan, R. van Beuningen, Nucleic Acids Res 32 (2004) e123.
[7] R. Hilhorst, L. Houkes, A. van den Berg, R. Ruijtenbeek, Anal. Biochem 387 (2009) 150–161.
[8] J.C. Miller, H. Zhou, J. Kwekel, R. Cavallo, J. Burke, E.B. Butler, B.S. Teh, B.B. Haab, Proteomics 3 (2003) 56–63.
[9] L.H. Mujawar, W. Norde, A. van Amerongen, Analyst 138 (2013) 518–524.
[10] L.H. Mujawar, A. van Amerongen, W. Norde, Talanta 98 (2012) 1–6.
[11] M. Reck, F. Stahl, J.G. Walter, M. Hollas, D. Melzner, T. Scheper, Biotechnol. Progr 23 (2007) 1498–1505.
[12] M. Dufva, Biomol. Eng 22 (2005) 173–184.
[13] J.-G. Walter, F. Stahl, M. Reck, I. Praulich, Y. Nataf, M. Hollas, K. Pflanz, D. Melzner, Y. Shoham, T. Scheper, Eng. Life Sci. 10 (2010) 103–108.
[14] J. Petrik, Transfusion Med 16 (2006) 233–247.
[15] T. Kukar, S. Eckenrode, Y. Gu, W. Lian, M. Megginson, J.-X. She, D. Wu, Anal. Biochem 306 (2002) 50–54.
[16] L. Mujawar, A. Moers, W. Norde, A. Amerongen, Anal. Bioanal. Chem 405 (2013) 7469–7476.
[17] B.A. Stillman, J.L. Tonkinson, BioTechniques (2000) 630–635.
[18] R.D. Deegan, Phys. Rev. E 61 (2000) 475.
[19] R.D. Deegan, O. Bakajin, T.F. Dupont, G. Huber, S.R. Nagel, T.A. Witten, Nature 389 (1997) 827–829.
[20] R.D. Deegan, O. Bakajin, T.F. Dupont, G. Huber, S.R. Nagel, T.A. Witten, Phys. Rev. E 62 (2000) 756.
[21] M.K. McQuain, K. Seale, J. Peek, S. Levy, F.R. Haselton, Anal. Biochem 320 (2003) 281–291.
[22] P. Wu, D.W. Grainger, J. Proteome Res 5 (2006) 2956–2965.
[23] F. Diehl, S. Grahlmann, M. Beier, J.D. Hoheisel, Nucleic Acids Res 29 (2001).
[24] Y. Deng, X.Y. Zhu, T. Kienlen, A. Guo, J. Am. Chem. Soc 128 (2006) 2768–2769.
[25] W. Norde, J. Lyklema, Adv. Colloid Interfac. 179–182 (2012) 5–13.
[26] M. Bohorquez, C. Koch, T. Trygstad, N. Pandit, J. Colloid Interfac 216 (1999) 34–40.
[27] P. Alexandridis, T. Alan Hatton, Colloid Surface A 96 (1995) 1–46.
[28] B. Fousseret, M. Mougenot, F. Rossignol, J.-F. Baumard, B. Soulestin, C. Boissière, F. Ribot, D. Jalabert, C. Carrion, C. Sanchez, M. Lejeune, Chem. Mater 22 (2010) 3875–3883.
[29] A. Kosmala, Q. Zhang, R. Wright, P. Kirby, Mater. Chem. Phy 132 (2012) 788–795.
[30] A. Wolter, R. Niessner, M. Seidel, Anal. Chem 79 (2007) 4529–4537.
[31] K.-H. Lee, J.-W. Lee, S.-W. Wang, L.-Y. Liu, M.-F. Lee, S.-T. Chuang, Y.-M. Shy, C.-L. Chang, M.-C. Wu, C.-H. Chi, J. Vet. Diagn. Invest. 20 (2008) 463–471.
[32] A. Isogai, M. Naito, Y. Ozaki, H. Nagashima, T. Enomae, J. Imaging Sci 55 (2011) (20201-20201-20201-20208).
[33] R.M.L. van Lieshout, T. van Domburg, M. Saalmink, R. Verbeek, R. Wimberger-Friedl, M.P. van Dieijen-Visser, C. Punyadeera, Anal. Chem 81 (2009) 5165–5171.
[34] L.H. Mujawar, A.A. Maan, M.K.I. Khan, W. Norde, A. van Amerongen, Anal. Chem 85 (2013) 3723–3729.
[35] V. Dugas, J. Broutin, E. Souteyrand, Langmuir 21 (2005) 9130–9136.
[36] A.K. Trilling, J. Beekwilder, H. Zuilhof, Analyst 138 (2013) 1619–1627.
[37] A. Mohammad Karim, H.P. Kavehpour, J. Coat. Technol. Res. (2013) 1–6.
[38] V.N. Luk, G.C.H. Mo, A.R. Wheeler, Langmuir 24 (2008) 6382–6389.
[39] M.E. Mohanty, V.J. Rao, A.K. Mishra, Spectrochim. Acta A 121 (2014) 330–338.
[40] A. Al-Nahain, S.Y. Lee, I. In, K.D. Lee, S.Y. Park, Int. J. Pharm 450 (2013) 208–217.
[41] Y. Zhao, D.Y. Alakhova, J.O. Kim, T.K. Bronich, A.V. Kabanov, J. Control. Release 168 (2013) 61–69.
[42] M.E. Wiseman, C.W. Frank, Langmuir 28 (2012) 1765–1774.
[43] M.R. Nejadnik, A.L.J. Olsson, P.K. Sharma, H.C. van der Mei, W. Norde, H. J. Busscher, Langmuir 25 (2009) 6245–6249.
[44] L.F. Pease, J.T. Elliott, D.-H. Tsai, M.R. Zachariah, M.J. Tarlov, Biotechnol. Bioeng 101 (2008) 1214–1222.
[45] W. Norde, D. Gage, Langmuir 20 (2004) 4162–4167.